

Stochastic Geometry Modeling for Uplink Cellular V2X Communication

Muhammad Nadeem Sial*, Yansha Deng*, *Member, IEEE*, Junaid Ahmed†, Arumugam Nallanathan‡, *Fellow, IEEE* and Mischa Dohler*, *Fellow, IEEE*

*Department of Informatics, King's College London, London, UK

† COMSATS Institute of Information Technology, Islamabad, Pakistan

‡Queen Mary University of London, London, UK

Abstract—To overcome the limitations of Dedicated Short Range Communications (DSRC) with short range, non-supportability of high density networks, unreliable broadcast services, signal congestion and connectivity disruptions, vehicle-to-everything (V2X) communication networks, standardized in 3rd Generation Partnership Project (3GPP) Release 14, have been recently introduced to cover broader vehicular communication scenarios including vehicle-to-vehicle (V2V), vehicle-to-pedestrian (V2P) and vehicle-to-infrastructure/network (V2I/N). Motivated by the stringent connection reliability and coverage requirements in V2X, this paper presents the first comprehensive and tractable analytical framework for the uplink performance of cellular V2X networks, where the vehicles can deliver their information via V2N/cellular network (vehicle-to-base station, V2B communication link) or directly between vehicles in the sidelink, based on their distances, propagation environments and the bias factor. By practically modeling the vehicles on the roads using the doubly stochastic Cox process and the BSs, we derive new association probabilities of V2B and V2V links, new success probabilities of the V2B and V2V communications, and overall success probability of the V2X communication, which are validated by the simulations results. Our results reveal the benefits of V2X communication compared to V2V communication in terms of success probability.

Index Terms—V2X communication, 5G, stochastic geometry, V2V, V2I, V2N, V2P, uplink cellular networks.

I. INTRODUCTION

VEHICLE-to-everything (V2X) communications based on cellular infrastructure have been defined by the Third Generation Partnership Project (3GPP) group [1] to cover broader spectrum of communication scenarios, such as vehicle-to-vehicle (V2V), vehicle-to-pedestrian (V2P) and vehicle-to-infrastructure/networks (V2I/N). It is regarded as a promising technology to support various novel applications such as road safety, infotainment services, traffic management, traffic optimization and online services to car manufacturers. Specifically, this innovation promises to eliminate 80% of the current road accidents and help in fostering auto-mobile and telecommunication industries for a smarter and safer ground transportation system [2].

Existing V2V communication can be supported via the DSRC standard, however, it has certain limitations such as short range, unable to support high density of networks and has unreliable broadcast services [3]. The underlying carrier sensing multiple access (CSMA) medium access control (MAC)

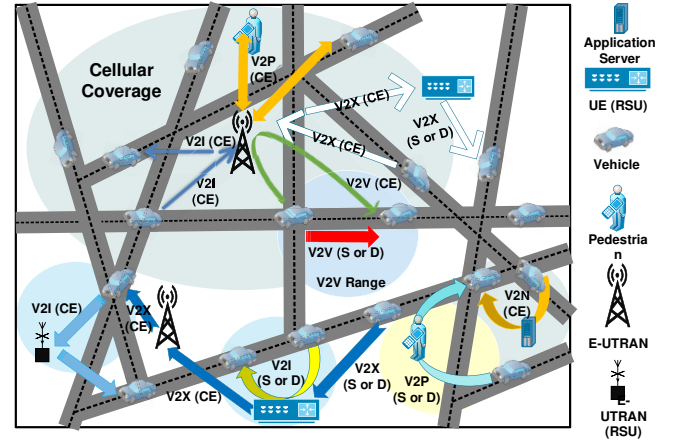


Fig. 1. V2X Communication scenarios.

protocol also exhibits signal congestion and connectivity disruptions due to rapid changing network topology and ad-hoc vehicular networks [4]. More importantly, single DSRC technology can not support a variety of incoming vehicular oriented applications, and only V2V and V2I communication is achievable using DSRC without the provisioning of V2P, infotainment and traffic management services.

To augment DSRC communication, V2X communication was proposed to meet V2X capacity, latency and coverage requirements [1], [3], [5] and [6] via operating in the following three scenarios as shown in Fig. 1. In V2X Scenario I, V2V, V2P or V2I messages are exchanged directly between vehicles without involvement of cellular nodes. In V2X Scenario II, V2V and V2P messages are first transmitted to the cellular node (eNB or E-UTRAN denoted as CE) in uplink, and then being forwarded to multiple vehicles at a local area in the downlink by cellular node. For V2I and V2N communications, the vehicle can communicate with the E-UTRAN type RSU and application server, respectively. In V2X scenario III (A), the vehicle first transmits the V2X message to UE type RSU which is further relayed to multiple vehicles through cellular node. In V2X scenario III (B), the V2X message is received by cellular node in the uplink and then transmitted to UE type RSU on downlink for further relaying it to multiple

vehicles. In all three scenarios, the vehicular communication can coexist with the cellular carriers called shared (S) or using dedicated carriers referred as dedicated channels (D). To model and analyze these V2X scenarios, stochastic geometry has been proposed, considering that it has been utilized as a powerful tool to model and analyze mutual interference between transceivers in the wireless networks, such as conventional cellular networks [7], [8], wireless sensor networks [9], cognitive radio networks [10], [11], and heterogeneous cellular networks [12]–[14].

The initial studies on vehicular communication have focused on modeling the V2V communication (i.e. without involvement of the cellular nodes) using stochastic geometry [15]–[22], where simple spatial models with a single road, a multi-lane road, or orthogonal roads were considered. The works in [23]–[28] accounted for the randomness of roads distributions. In [23], the nodes in the WiFi mesh networks were modeled by a Cox process on a Poisson-Line tessellation (PLT), and the nodes on each line are modeled by a inhomogeneous 1D PPP, where the probability density function of the shorted Euclidean distance between two inter-nodes was derived. Later on in [24], the Cox process on a PLT was generalized to a Poisson-Line tessellation (PLT), Poisson-Voronoi tessellation (PVT), or a Poisson-Delaunay tessellation (PDT), and the nodes on each line are modeled by a homogeneous 1D PPP. Their results have shown that PLT often gains preference over PVT and PDT in modeling road systems¹ due to its analytical tractability. In [25], the uplink coverage probability was derived for a network where the typical receiver is randomly chosen from a PPP, and the locations of transmitter mobile users alongside roads are modeled as a Cox process on a Poisson line process (PLP). In [28], the coverage probability of the V2V communication was derived, where the transmitters and receivers were modeled using independent Cox processes on the same PLP (i.e. a doubly-stochastic spatial model), and it captures the irregularity in the spatial layout of roads via the PLP model, and the distribution of vehicles on each road via the 1D PPP model.

Note that [23]–[28] are limited to the V2V communication or V2I communication. The first performance characterization of the V2X downlink communication was studied in the master thesis in [30], where the association probabilities and the coverage probabilities for the V2V and the base station to vehicle downlink communications were derived for the maximum power based association scheme and the threshold distance based association scheme. Recently, [31] has performed downlink coverage analysis of cellular network leveraging vehicles where authors have derived the distance of typical receiver vehicle at center from nearest base station or vehicle. Further, they derived downlink association and the coverage probabilities of the typical vehicle in terms of integral formulas to characterize the downlink performance of vehicular communication. However, in these works, uplink performance or association probabilities have not been studied. Moreover, authors have not suggested any mechanism during association process to control vehicular communication over

cellular network to limit interference on cellular users.

The present paper can be seen as an extension to downlink communication work presented in [30], [31]. In this paper, we focus on the uplink communication of V2X networks driven by the stringent high reliability requirements for safety, traffic management and infotainment applications where the locations of vehicles are modeled as a Cox process on a Poisson Line Process (PLP), and the cellular BSs are deployed as 2D PPP. A flexible V2X uplink selection scheme is proposed to control the amount of vehicular interference and the number of vehicles operating on the cellular band which has not been previously presented in the existing literature. Our contributions can be summarized as follows:

- We present a comprehensive and tractable analytical framework for analyzing the uplink communication of cellular V2X networks, where the vehicles decide to transmit to other vehicle or cellular BS via shared carriers depending on their corresponding distances, propagation environments and association bias.
- Based on the proposed V2X link selection scheme, we derive the shortest distances and the association probabilities of the vehicles using the V2V link or the V2B link via the shared cellular carriers, respectively.
- We derive the analytical expressions for the success probabilities of the V2V communication and the V2B communication, and the overall success probability of typical vehicle (i.e., V2X communication) using the uplink cellular resources, which are validated by Monte Carlo simulation.
- In V2X network with low and medium vehicle intensity on the roads, there is almost equal probability of transmitting via the V2V and the V2B link. Moreover, cellular based V2V link success probability increases at faster rate with the increase of vehicle nodes, and the success probability of the V2X communication improves with increasing the road intensity
- Our results have shown that the success probability of the V2X communication is much higher than that of the V2V communication, as both cellular based V2V and V2B links supplement each other to achieve higher success probability of V2X communication.

The rest of the paper is organized as follows. The mathematical preliminary, system model along with assumptions, and the methodology of analysis are described in Section II and III, respectively. Section IV presents the analysis of association probabilities of V2X communication. The success probability is analyzed in Section V. Section VI presents and discusses the numerical and simulation results. The paper is concluded in Section VII. A list of the key mathematical notations used in this paper is given in Table I.

II. PRELIMINARY: POISSON LINE PROCESS

The V2X networks exhibit unique spatial characteristics due to the fact that vehicles are only driven on roadways, which are predominantly linear in nature and layout of the roads is often irregular, which makes it possible to model the road system as a realization of a line process [22]–[25], [28],

¹ It has also been used in other related applications, such as in modeling the effect of blockages in localization networks [29].

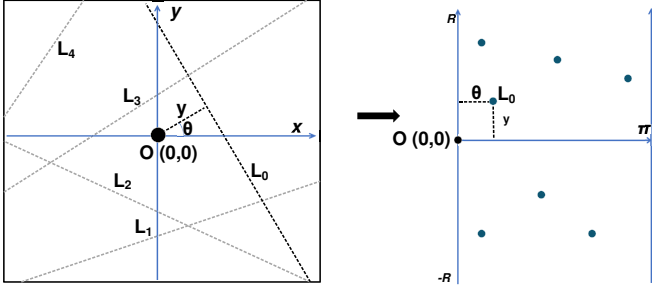


Fig. 2. (a) Illustration of Poisson Line Process in two dimensional plane \mathbb{R}^2 (left). (b) Illustration of Poisson Process on representation space $\mathbb{C} = [0, 2\pi) \times [0, \infty)$ (right).

[32]. Therefore, we model the roadways as a network of lines that are distributed on the plane according to a Poisson Line Process (PLP). In this section, we provide a brief introduction of PLP, the detailed information of the underlying theory can be found in [28], [30], [33].

A Poisson line process is a random collection of lines in a 2D plane. Any undirected line L in \mathbb{R}^2 can be uniquely characterized by its perpendicular distance y from the origin $O(0,0)$ and the angle θ subtended by the perpendicular dropped onto the line from the origin with respect to the positive x-axis in counter clockwise direction, as shown in Fig. 2. The pair of parameters θ and y can be represented as the coordinates of a point on the cylindrical surface $\mathbb{C} = [0, 2\pi) \times [0, \infty)$ as illustrated in Fig. 2. Clearly, there is a one-to-one correspondence between the lines in \mathbb{R}^2 and points on the cylindrical surface \mathbb{C} . Thus, a random collection of lines can be constructed from a set of points on \mathbb{C} . In other words, the set of points generated by a PPP with certain density on \mathbb{C} correspond to the PLP with the same density for lines on \mathbb{R}^2 .

For a PLP ϕ_R with the intensity λ_R within a circular region $\mathcal{B}(0, R)$, where radius $R \in \mathbb{R}$, the corresponding points are independent and uniformly distributed in representation space $\mathbb{C} = [-R, R] \times [0, \pi]$ with a surface area of $2\pi R$. Thus, the expected number of points in the PPP that lie in \mathbb{C} is $2\pi\lambda_R R$, and the number of lines intersecting a disc of radius R is a Poisson distributed with mean $2\pi\lambda_R R$. In PLP, the values of θ and y of each line follow a uniform distribution over an appropriate range defined by \mathbb{C} . In this work, we limit ourselves to motion-invariant PLP, where the line process is invariant to the rotation of axes to the origin, for analytical simplicity [28]. The PLP is also considered to be stationary, where translated line process $T\phi_R = \{T(L_1), T(L_2), \dots\}$ of PLP, $\phi_R = \{L_1, L_2, \dots\}$ has the same distribution of lines as that of ϕ_R for any translation T in the plane [28].

III. SYSTEM MODEL

In this work, we consider a cellular V2X networks with coexistence of V2V, V2P and V2I/N communications as per scenario I and II defined by 3GPP Release 14 and shown in Fig. 1. In this scenario, V2V, V2P and V2I/N messages are exchanged in uplink and downlink for the applications like vehicular safety. The system model are described in detail in the following subsections.

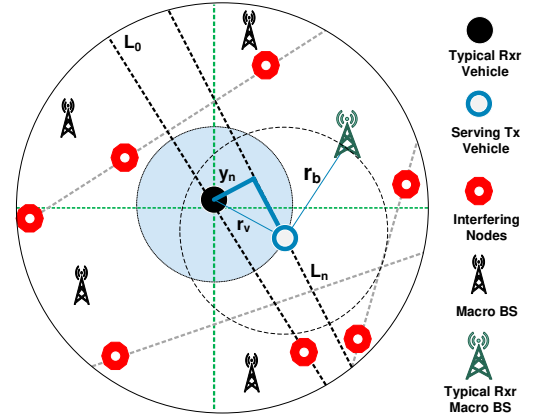


Fig. 3. Illustration of the system model.

A. V2X Vehicular Nodes

As mentioned in Section II, we model the roads as motion-invariant PLP ϕ_R with line intensity, λ_R as per details given in [28], [30], [31], thus the intensity of equivalent Poisson Point Process (PPP) on the representation space \mathbb{C} is λ_R . The V2X vehicular nodes are randomly distributed on each road as homogeneous 1D PPP with intensity μ_v . In this paper, we only distribute the V2X vehicular nodes to derive the basic analytical framework which can be further extended by including pedestrian and RSUs by distributing them according to independent PPP's of intensities μ_p and μ_r , respectively as discussed by [28], [30]. However, the pedestrian near roadside and RSUs will have channel conditions different from vehicular nodes due to varying antenna heights.

Assuming that each vehicle transmits independently with a probability p , the locations of transmitting vehicles on each road is then given by a thinned PPP with intensity, $\mu_t = p\mu_v$, and we denote the set of locations of the transmitting vehicles on a line L by W_L . Correspondingly, the distribution of receiving vehicles on each line is also a thinned PPP with intensity, $\mu_r = (1-p)\mu_v$. In other words, the transmitting and receiving vehicles are modeled as the doubly stochastic processes called Cox processes, ϕ_t and ϕ_r , which are driven by the same PLP, ϕ_R .

For analytical simplicity, we can translate the origin $O = (0,0)$ to the location of the typical receiver vehicle. The translated point process ϕ_{r_0} can be treated as the superposition of the point process ϕ_r , an independent 1D PPP with intensity μ_r on a line passing through the origin and a vehicle at the origin O . This can be realized according to the following steps defined by [28]. We first add a point at the origin to the PPP in the representation space \mathbb{C} by applying the Slivnyak's theorem [33], thereby obtaining a PLP $\phi_{R_0} = \phi_R \cup L_0$ with a line L_0 passing through the origin in \mathbb{R}^2 and second, we add a point at the origin to the 1D-PPP on the line L_0 passing through the origin in \mathbb{R}^2 by applying the Slivnyak's theorem [33]. The line, L_0 passing through the origin is referred as typical line in this paper. Since, both ϕ_t and ϕ_r are driven by the same line process, the translated point process ϕ_{t_0} is also the superposition of ϕ_t and an independent PPP with intensity μ_t

TABLE I
NOTATIONS

Notations	Definition
λ_R	Intensity of roads, 2D PLP
μ_v	Intensity of V2X nodes, ID PPP
λ_b	Intensity of base-stations, 2D PPP
ϕ_R	Poisson Line Process (PLP) for roads
ϕ_t	Cox process for transmitting nodes
ϕ_r	Cox process for receiving nodes
ϕ_b	2D PPP for cellular base-stations
B	Association bias, 0 to ∞
P_b	Base-station transmit power
P_v	Vehicle transmit power
α_v	Path loss exponent for V2V link
α_b	Path loss exponent for V2B link
y_n	Perpendicular distance of road from origin
θ	Angle of road from x-axis
BW	V2X communication channel bandwidth, 10 MHz
V2V	Vehicle to vehicle uplink
V2B	Vehicle to base-station uplink
r_v	V2V distance
r_b	V2B uplink distance
r_{b2v}	B2V downlink distance
σ^2	Thermal noise

on L_0 . Note that the other receiving vehicles in the network do not interfere with the typical receiving vehicle in our setup, therefore, we focus only on the distribution of transmitting vehicles. In this work, the impact of the vehicle mobility and direction are neglected, similar to the work presented by [31], [34].

B. Cellular Base Stations

We consider the cellular BSs are spatially distributed in \mathbb{R}^2 according to the 2D PPP with intensity λ_b . This model for macro BSs has been validated to be as accurate to the typical hexagonal grid model [35]. We assume that each base-station will always have at least one V2X node connected with the BS in the uplink. Due to the shared spectrum between the V2V communication and the V2B communication, there will exist interference between them.

C. V2X Uplink Selection

In our model, the vehicles transmit with the fixed power P_v . The link selection between V2V and V2B communication is determined by the corresponding distances, propagation environments and association bias factor B to limit interference and traffic on cellular network. In other words, it can tune the trade-off interference and data offloading [36]. In this flexible V2X link selection scheme, the vehicle selects the V2V link if $B r_v^{-\alpha_v} \geq r_b^{-\alpha_b}$, otherwise the vehicle selects the V2B link, where r_v is the shortest V2V link distance, and r_b is the distance between the V2X node and its closest cellular BS. For the extreme case with $B = 0$, the V2V link will never be selected, whereas for the case with $B = \infty$, each vehicle transmitter always selects the V2V link. It is worth mentioning that one main advantage of this link selection criterion is that it brings an inherent interference protection to the cellular uplink, which is necessarily required to enable shared link in cellular networks.

D. Channel Model

A general power-law path-loss model is considered in which the signal power decays at the rate, $r^{-\alpha}$ with the propagation distance r , where α is the path-loss exponent. Due to the different propagation environments experienced in the V2B and V2V links, each type of link is given its own path-loss exponent, namely, α_b and α_v , respectively. The small-scale channel fading is modeled as slow-flat Rayleigh fading as used by [17], [21], [30], [31], [34], [36], where its channel gain is assumed to be exponentially distributed with unit mean. All the channel gains are assumed to be independent of each other, independent of the spatial locations, symmetric, and are identically distributed (i.i.d.). We use Rayleigh fading for V2B and V2V links for its analytical tractability and this assumption is also the most popular in the literature to get closed-form expressions [11]. However, the analytical expressions can be easily extended to interesting scenarios such as non-exponential fading [31]. For log normal shadowing, we have included the shadowing in a transparent way by using the displacement theorem given by [37] and method described by [38].

E. V2X Communication Reliability or Success Probability

The transmitting vehicle connects to a receiver (either BS or vehicle) depending on the corresponding distances, propagation environments and association bias, and thus the transmitting vehicle can operate in modes $M \in \{v2b, v2v\}$, where $v2b$ and $v2v$ modes denote the shared link communication between vehicle and cellular BS and that between vehicle and vehicle, respectively. The success probability (reliability) of the typical receiver (base-station or vehicle) conditioned on minimum distance r between transmitter and receiver and mode M can be defined as the probability that the SINR of receiver is greater than a SINR Threshold, z , which is given as

$$P_M^S(z|r, M) = \Pr[SINR > z] = \Pr\left[\frac{Pr^{-\alpha}h}{I + \sigma^2} > z\right], \quad (1)$$

where P is transmit power, h is channel gain and r is the minimum distance between transmitter and the receiver. Note that the transmitting vehicle always connects to typical receiver (BS or vehicle) at distance r , thus there will be no interfering vehicles present in the disk $\mathcal{B}(0, r)$ with radius r as shown in Fig. 3. The size of $\mathcal{B}(0, r)$ affects the distribution of interfering nodes, Φ_I as well as the interference to typical receiver. We need to characterize the distribution of interferers, Φ_I as per their locations (interferers located on road passing through origin or on all other roads) to determine the Laplace transform of the distribution of interference power conditioned on the serving distance r and mode M .

Remind that r is the minimum possible distance between the receiver and transmitter, and the interfering vehicles are located outside the disk $\mathcal{B}(0, r)$. Therefore, the interferers can be broadly divided into two categories, (a) the interfering vehicles that are located outside the disk $\mathcal{B}(0, r)$ on the road passing through the origin and (b) the interfering vehicles located outside the disk $\mathcal{B}(0, r)$ on all other roads. The

distribution of interferers located on all other roads can be denoted as $\Phi_v|\mathcal{B}(0, r)$ and the disk $\mathcal{B}(0, r)$ does not contain any interfering vehicles. Similarly, the distribution of interferers located on road passing through the origin can be denoted as $\Phi_r|r$ and there are no vehicles on the road segment from 0 to $2r$ for road passing through origin. As such, the success probability can be rewritten as

$$P_M^S(z|r, M) = \Pr \left[\frac{Pr^{-\alpha}h}{I_v + I_r + \sigma^2} > z \right], \quad (2)$$

where σ^2 is the thermal noise power, I_v and I_r are the aggregate interference due to the vehicles located on all other roads, and on the road passing through the origin that operate in mode $v2b$ or $v2v$, respectively.

IV. ASSOCIATION PROBABILITIES

To facilitate the reliability analysis of proposed V2X networks, we first derive the distance distributions of the V2V link and the V2B link, and their corresponding association probability in the following.

Lemma 1 (V2V Distance): The CDF of the shortest distance R_v between the vehicular transmitter and a typical vehicular receiver in the V2V link, $F_{R_v}(r_v)$ is given in [30], we still present results below for completeness

$$F_{R_v}(r_v) = 1 - \left[\exp \left(-2\pi\lambda_R \int_{y_n=0}^{r_v} 1 - e^{-2\mu_v\sqrt{r_v^2 - y_n^2}} dy_n \right) \times \exp(-2\mu_v r_v) \right]. \quad (3)$$

Corollary 1 (The PDF of V2V Link): The Probability Density Function (PDF), $f_{R_v}(r_v)$ of the shortest distance between the vehicular transmitter and a typical vehicular receiver, R_v in the V2V link is derived as

$$f_{R_v}(r_v) = \left(-4\pi\lambda_R\mu_v \int_0^{r_v} \frac{r_v e^{-2\mu\sqrt{r_v^2 - y_n^2}}}{\sqrt{r_v^2 - y_n^2}} dy_n - 2\mu_v \right) \times \left[-\exp \left(-2\pi\lambda_R \int_0^{r_v} \left(1 - e^{-2\mu_v\sqrt{R^2 - r^2}} \right) dy_n - 2r_v\mu_v \right) \right]. \quad (4)$$

Proof 1: The Probability Density Function (PDF) of R_v can be found by taking derivative of CDF given in Eq. (3), $f_{R_v}(r_v) = \frac{d}{dr_v}(F_{R_v}(r_v))$ and final result for PDF of R_v is given as Eq. (4). The closed form solution of Eq. (4) is derived as

$$f_{R_v}(r_v) = \left(-2\pi^2\lambda_R r_v \mu_v \left[I_0(2r_v\mu_v) - L_0(2r_v\mu_v) \right] - 2\mu_v \right) \times \left[-\exp \left(-2\pi\lambda_R r_v + \pi^2\lambda_R r_v \left[L_{-1}(2r_v\mu_v) - I_1(2r_v\mu_v) \right] - 2r_v\mu_v \right) \right], \quad (5)$$

where $I_n(z)$ ($n = 0, 1$) denotes the modified Bessel functions of the first kind and $L_n(z)$ ($n = 0, -1$) denotes the modified Struve functions. This completes the proof.

Lemma 2 (V2B Distance): The PDF of the distance between a vehicular transmitter and the nearest BS, R_B for the shared link $f_{R_B}(r_b)$ is given in [7, Eq. (2)] as

$$f_{R_b}(r_b) = 2\pi\lambda_b r_b e^{-\pi\lambda_b r_b^2}. \quad (6)$$

According to the flexible V2X link selection scheme proposed in section III, the vehicle selects the V2V link if $B r_v^{-\alpha_v} \geq r_b^{-\alpha_b}$, otherwise the vehicle selects the V2B link, where r_v is the shortest V2V link distance, and r_b is the distance between the transmitting vehicle and its closest cellular BS. Therefore, the vehicular transmitter can connect with the vehicular receiver or BS in the uplink with their corresponding association probabilities. In Lemma 3 and Lemma 4, we derive the association probabilities of the V2V link and the V2B link, respectively.

Lemma 3 (Association probability of the V2V Link): The probability of the vehicular transmitter selecting the V2V link is derived as

$$P_{v2v}^A = \int_0^\infty -\exp \left(-2\pi\lambda_R r_v + \pi^2\lambda_R r_v \left[L_{-1}(2r_v\mu_v) - I_1(2r_v\mu_v) \right] - 2r_v\mu_v \right) \times \left(-2\pi^2\lambda_R r_v \mu_v \left[I_0(2r_v\mu) - L_0(2r_v\mu_v) \right] - 2\mu_v \right) \times \exp \left(-\pi\lambda_B \left(\frac{r_v^{\frac{\alpha_v}{\alpha_b}}}{B^{\frac{1}{\alpha_b}}} \right)^2 \right) dr_v, \quad (7)$$

where λ_B is the cellular base-station intensity, μ_v is the V2X nodes intensity, λ_R is the road intensities, B is the association bias, $I_n(z)$ ($n = 0, 1$) is the modified Bessel functions of the first kind, and $L_n(z)$ ($n = 0, -1$) is the modified Struve functions.

Proof 2: See Appendix A.

Lemma 4 (Association probability of the V2B Link): The probability of the vehicular transmitter selecting V2B link is derived as

$$P_{v2b}^A = \int_0^\infty \exp \left[-2\pi\lambda_R \times \int_{y_n=0}^{B^{\frac{1}{\alpha_v}} r_b^{\frac{\alpha_b}{\alpha_v}}} 1 - \exp \left(-2\mu_v \times \sqrt{\left(B^{\frac{1}{\alpha_v}} r_b^{\frac{\alpha_b}{\alpha_v}} \right)^2 - y_n^2} \right) \times dy_n \right] \times \exp \left(-2\mu_v B^{\frac{1}{\alpha_v}} r_b^{\frac{\alpha_b}{\alpha_v}} \right) \times 2\pi\lambda_b r_b \exp[-\pi\lambda_b r_b^2] dr_b \quad (8)$$

where λ_B is the cellular base-station intensity, μ_v is the V2X nodes intensity, λ_R is the road intensities, B is the association bias.

Proof 3: See Appendix B.

V. V2X SUCCESS PROBABILITY

In this section, we derive the success probability of the V2X communication. To do so, we first need to characterize the interference from each type of interferer category (I_v, I_r). Thus, we calculate the general form of Laplace Transform, and we derive the expressions of Laplace Transform of interference from I_v and I_r in this section.

A. Laplace Transform of Interference Under Rayleigh Fading

As we know that Laplace Transform of interference, I_X is $\mathcal{L}_{I_X}(s) = E_{I_x} [e^{-sI_x}]$. The interfering set of vehicles X for each category of interfering vehicles (I_v, I_r) based on their location can be represented as

$$I_X = \sum_{x \in X} P_v h_x D_x^{-\alpha}, \quad (9)$$

where X represent various interference sources (I_v, I_r) and P_v is the transmit power of the vehicle. For a vehicle $x \in X$, we denote its distance to the typical receiver as D_x . Although the random variables $[D_x]_{x \in X}$, are identically distributed, they are not independent in general [7]. However, authors in [7] have shown that this dependence is weak and we will henceforth, assume each D_x to be i.i.d. Due to the different propagation environments experienced in the V2B and V2V links, each type of link will have its own path-loss exponent and α can be replaced with α_b or α_v in (9) as per selected link. The expression for $\mathcal{L}_{I_X}(s)$ is given as

$$\mathcal{L}_{I_X}(s) = \mathbb{E}_{I_X} \left[e^{-\sum_{x \in X} s P_v h_x D_x^{-\alpha}} \right]. \quad (10)$$

By taking expectation over h_x, D_x , we get

$$\mathcal{L}_{I_X}(s) = \mathbb{E}_{h_x, D_x} \left[\prod_{x \in X} \exp(-s P_v h_x D_x^{-\alpha}) \right]. \quad (11)$$

By assuming all h_x as independent, we obtain

$$\mathcal{L}_{I_X}(s) = \mathbb{E}_{D_x} \left[\prod_{x \in X} E_{h_x} [\exp(-s P_v h_x D_x^{-\alpha})] \right]. \quad (12)$$

Based on the fact that $h \sim \exp(1)$, we obtain

$$\mathcal{L}_{I_X}(s) = \mathbb{E}_{D_x} \left[\prod_{x \in X} \left[\frac{1}{1 + s P_v R_x^\alpha D_x^{-\alpha}} \right] \right]. \quad (13)$$

Now, we calculate the Laplace transform of interference for each category of road (I_v and I_r) in the following. Let us denote the outer circular region in which all roads exist as $\mathcal{B}(0, R)$, and inner circular region $\mathcal{B}(0, r)$ with radius r having minimum distance between transmitter and receiver as shown in Fig. 3. Let us denote two types of road as R_{in} and R_{out} , where R_{in} are the roads intersecting the circular region $\mathcal{B}(0, r)$, and R_{out} are the roads that lie outside the circular region $\mathcal{B}(0, r)$ and within circular region $\mathcal{B}(0, R)$. Thus, road R_{in} is located at distance, $y < r$ and in case of R_{out} , it is located at distance $y > r$. In this case, the interferers can be located anywhere on road R_{out} as it is located outside $\mathcal{B}(0, r)$. However, in case of R_{in} , the interferers will be located in regions between $(-\sqrt{R^2 - y^2}, -\sqrt{r^2 - y^2})$ and

$(\sqrt{R^2 - y^2}, \sqrt{r^2 - y^2})$. In the following, we calculate the Laplace Transform for the interferences from the vehicular transmitters located in these two types of roads (i.e., R_{in} and R_{out}).

Corollary 2 (Laplace Transform of Interference for Single Road Located Outside Inner Circular Region, $\mathcal{B}(0, r)$): The conditional Laplace transform of interference at typical receiver, originating from a single road located at a distance y ($y > r$), outside inner circular region, $\mathcal{B}(0, r)$ with radius r is expressed as

$$\mathcal{L}_{I_{R_{out}}}(s|r) = \exp \left[-2\mu_v \int_0^\infty \left[1 - \frac{1}{1 + s P_v (y^2 + t^2)^{\frac{-\alpha}{2}}} \right] dt \right]. \quad (14)$$

For $\alpha = 4$, the closed form solution can be simplified as

$$\mathcal{L}_{I_{R_{out}}}(s|r) = \exp \left(-\mu_v \frac{\pi r^2 \sin \left(\frac{1}{2} \tan^{-1} \left(\frac{r^2}{y^2 \sqrt{\frac{1}{z}}} \right) \right)}{\sqrt{\frac{1}{z}} \sqrt[4]{y^4 + r^4 z}} \right). \quad (15)$$

Proof 4: See Appendix C.

Corollary 3 (Laplace Transform of Interference for Single Road Intersecting the Inner Circular Region, $\mathcal{B}(0, r)$): The conditional Laplace transform of interference at typical receiver, originating from a single road located at distance y ($y < r$), intersecting the inner circular region, $\mathcal{B}(0, r)$ with radius r is derived as

$$\mathcal{L}_{I_{R_{in}}}(s|r) = \exp \left[-2\mu_v \int_{\sqrt{r^2 - y^2}}^\infty \left(1 - \frac{1}{1 + s P_v (y^2 + t^2)^{\frac{-\alpha}{2}}} \right) dt \right]. \quad (16)$$

Proof 5: For this case, the value of t varies from $t = (-\sqrt{r^2 - y^2})$ to $(\sqrt{r^2 - y^2})$ and the range of region in which the interfering nodes will be located is $(-\infty, -\sqrt{r^2 - y^2})$ and $(\sqrt{r^2 - y^2}, \infty)$. Therefore, the Laplace Transform of interference can be calculated by changing the limits of Eq. (14) and is given as Eq. (16). This completes the proof.

Based on the results in Corollary 2 and 3, we can derive the Laplace transform of the interference from the vehicles located on the road passing through the origin and that located on all other roads in Corollary 4 and 5, respectively.

Corollary 4 (Laplace Transform of Interference from Vehicles Located on Road Passing Through Origin): The conditional Laplace transform of interference at typical receiver, originating from road located at a distance of $y = 0$ is derived as

$$\mathcal{L}_{I_r}(s|r) = \exp \left[-\frac{2 \times r \times z \times \mu_v \times {}_2F_1 \left(1, \frac{\alpha-1}{\alpha}, 2 - \frac{1}{\alpha}, -z \right)}{\alpha-1} \right], \alpha > 1. \quad (17)$$

where ${}_2F_1(a, b, c, z)$ is the Hypergeometric function and z is the SINR threshold. For $\alpha = 4$, the closed form expression for the above equation is simplified as

$$\mathcal{L}_{I_r}(s|r) = \exp \left[-\frac{r \times \sqrt[4]{z} \mu_v}{\sqrt{2}} \times \left(-\tan^{-1} \left(\frac{\sqrt{2}}{\sqrt[4]{z}} + 1 \right) + \tan^{-1} \left(1 - \frac{\sqrt{2}}{\sqrt[4]{z}} \right) - \coth^{-1} \left(\frac{\sqrt{z} + 1}{\sqrt{2} \sqrt[4]{z}} \right) + \pi \right) \right]. \quad (18)$$

Proof 6: The conditional Laplace transform of interference can be calculated using Corollary 3 and $y = 0$, and the resultant equation is derived as

$$\mathcal{L}_{I_r}(s|r) = \exp \left(-2\mu_v \int_r^\infty \left[1 - \frac{1}{1 + sP_v t^{-\alpha}} \right] dt \right). \quad (19)$$

The closed form solution of Eq. (19) for all values of α is proved in (17).

Corollary 5 (Laplace Transform of Interference from All Roads Excluding Road Passing Through Origin): The conditional Laplace transform of the total interference at the typical receiver, originating from vehicular transmitters located on all roads except the road passing through the origin is derived as

$$\mathcal{L}_{I_v}(s|r) = \left[\exp \left(2\mu_v \lambda_R \int_0^r 1 - \mathcal{L}_{I_{R_{in}}}(s) dy \right) \right] \times \left[\exp \left(2\mu_v \lambda_R \int_r^R 1 - \mathcal{L}_{I_{R_{out}}}(s) dy \right) \right], \quad (20)$$

where $\mathcal{L}_{I_{R_{in}}}(s)$ and $\mathcal{L}_{I_{R_{out}}}(s)$ are given in (16) and (14), respectively.

Proof 7: See Appendix D.

With the help of Corollary 4 and 5, we can derive the success probabilities for the V2V link and that for the V2B link for a given distance r in the following theorems.

Theorem 1 (Success Probability of the V2V Shared Link): The success probability of the V2V link for given minimum distance r_v between transmitter and receiver is derived as

$$P_{v2v}^S(z|r_v) = \exp \left(-\frac{z\sigma^2}{P_v r_v^{-\alpha_v}} \right) \mathcal{L}_{I_v} \left(\frac{z}{P_v r_v^{-\alpha_v}} | r_v \right) \times \mathcal{L}_{I_r} \left(\frac{z}{P_v r_v^{-\alpha_v}} | r_v \right), \quad (21)$$

where $\mathcal{L}_{I_v}(s|r_v)$ and $\mathcal{L}_{I_r}(s|r_v)$ are given in Eqs. (17) and (20) by substituting $s = \frac{z}{P_v r_v^{-\alpha_v}}$.

Proof 8: The success probability of the V2V shared link for given minimum distance, r_v between transmitter and receiver and operating mode $M = v2v$ is

$$P_{v2v}^S(z|r_v) = Pr[SINR > z]. \quad (22)$$

Using Eq. (2), the above equation can be written as

$$P_{v2v}^S(z|r_v) = Pr \left[\frac{P_v r_v^{-\alpha_v} h}{I_v + I_r + \sigma^2} > z \right]. \quad (23)$$

With mathematical simplification, the final equation for the success probability of the V2V link for given minimum distance, r_v between transmitter and receiver is proved in Eq. (21).

Theorem 2 (Uplink Success Probability for the V2B Link): The uplink success probability for the V2B shared link for given minimum distance, r_b between transmitter and receiver is derived as

$$P_{v2b}^S(z|r_b) = \exp \left(-\frac{z\sigma^2}{P_v \times r_b^{-\alpha_b}} \right) \times \mathcal{L}_{I_v} \left(\frac{z}{P_v \times r_b^{-\alpha_b}} | r_b \right) \times \mathcal{L}_{I_r} \left(\frac{z}{P_v \times r_b^{-\alpha_b}} | r_b \right). \quad (24)$$

where $\mathcal{L}_{I_v}(s|r_b)$ and $\mathcal{L}_{I_r}(s|r_b)$ are given in Eqs. (17) and (20) by substituting $s = \frac{z}{P_v r_b^{-\alpha_b}}$.

Proof 9: The success probability for the V2B link for given minimum distance, r_b between transmitter and receiver is presented as

$$P_{v2b}^S(z|r_b) = P[SINR > z]. \quad (25)$$

By using Eq. (2), the above equation can be written as

$$P_{v2b}^S(z|r_b) = Pr \left[\frac{P_v r_b^{-\alpha_b} h}{I_v + I_r + \sigma^2} > z \right]. \quad (26)$$

With mathematical simplification, the final equation for the success probability of the V2B link for given minimum distance, r_b between transmitter and receiver is proved in Eq. (24).

Corollary 6 (Success Probability of Cellular V2X Network): The success probability of cellular V2X network is derived as

$$P_{V2X}^S(z) = \int_0^\infty \exp \left(-\frac{z\sigma^2}{P_v \times r_v^{-\alpha_v}} \right) \times \mathcal{L}_{I_v} \left(\frac{z}{P_v \times r_v^{-\alpha_v}} | r_v \right) \times \mathcal{L}_{I_r} \left(\frac{z}{P_v \times r_v^{-\alpha_v}} | r_v \right) \times P_{v2v}^A(v2v|r_v) \times f_{R_v}(r_v) dr_v + \int_0^\infty \exp \left(-\frac{z\sigma^2}{P_v \times r_b^{-\alpha_b}} \right) \times \mathcal{L}_{I_v} \left(\frac{z}{P_v \times r_b^{-\alpha_b}} | r_b \right) \times \mathcal{L}_{I_r} \left(\frac{z}{P_v \times r_b^{-\alpha_b}} | r_b \right) \times P_{v2b}^A(v2b|r_b) \times f_{R_b}(r_b) \times dr_b, \quad (27)$$

where $\mathcal{L}_{I_v}(s|r)$ and $\mathcal{L}_{I_r}(s|r)$ are given in Eqs. (17) and (20) by substituting $s = \frac{z}{P_v r^{-\alpha}}$ and $r = r_v$ or $r = r_b$ and $\alpha = \alpha_b$ or $\alpha = \alpha_v$. The $P_{v2v}^A(v2v|r_v)$ is given in Eq. (32), and $P_{v2b}^A(v2b|r_b)$ is given in Eq. (37).

Proof 10: By using total probability law, the success probability of V2X network is

$$P_{V2X}^S(z) = P_{v2v}^S(z|r_v) \times P_{v2v}^A(v2v|r_v) + P_{v2b}^S(z|r_b) \times P_{v2b}^A(v2b|r_b), \quad (28)$$

where $P_{v2v}^S(z|r_v)$ is given in Eq. (21), $P_{v2b}^S(z|r_b)$ is given in Eq. (24), $P_{v2v}^A(v2v|r_v)$ is given in Eq. (32) and $P_{v2b}^A(v2b|r_b)$ is given in Eq. (37). By removing the distance (r_v and r_b)

condition on Eq. (28), the V2X overall success probability is proved in Eq. (27), which completes the proof.

For the purpose of comparison, we derive the success probability of vehicular communication without involvement of cellular network in the following:

Corollary 7 (Success Probability of the V2V Communication without Cellular Network): The success probability of V2V Communication without cellular network is derived as

$$P_{v2v}^{only}(z) = \int_0^{\infty} \exp\left(-\frac{z\sigma^2}{P_v \times r_v^{-\alpha_v}}\right) \times \mathcal{L}_{I_v}\left(\frac{z}{P_v \times r_v^{-\alpha_v}}|r_v\right) \times \mathcal{L}_{I_r}\left(\frac{z}{P_v \times r_v^{-\alpha_v}}|r_v\right) \times f_{R_v}(r_v) \times dr_v, \quad (29)$$

where the PDF of r_v is given in Eq. (4), and $\mathcal{L}_{I_v}(s|r_v)$ and $\mathcal{L}_{I_r}(s|r_v)$ are given in Eqs. (17) and (20) by substituting $s = \frac{z}{P_v r_v^{-\alpha_v}}$.

Proof 11: The success probability of V2V Communication without cellular network can be derived by removing condition on r_v in Eq. (21) and the final expression is proved in Eq. (29).

VI. NUMERICAL RESULTS

In this section, the association probability of V2V link, association probability of V2B link, and the success probability are plotted using (7), (8), and (27), respectively. We also plot the success probability of the cellular based V2V and V2B link along with its association probability using the first part of Eq. (27), and the second part of Eq. (27), respectively. The analytical results are validated by Monte Carlo simulations as shown in each figure. In all the figures, we set the path loss at $\alpha_v = \alpha_b = 4$ and the thermal noise spectral density, $\sigma^2 = -174$ dBm/Hz for 10 MHz bandwidth. The transmit power of vehicles are set to be 23 dBm as defined by [1]. For comparison purposes, only V2V communication without cellular networks has also been plotted using (29) to exhibit advantages of cellular V2X communication over V2V communication. In the figures, ‘‘analyt. represents analytical plot, ‘‘sim’’ represents simulation plot, ‘‘C-V2V’’ represents cellular based V2V communication, ‘‘C-V2B’’ represents cellular based V2B communication, ‘‘V2X’’ represents cellular V2X communication, and ‘‘V2V’’ represents V2V communication without cellular. Note, cellular based V2V communication (C-V2V) is different from V2V communication without cellular as it involves V2V association probability depending upon V2X link selection scheme.

A. Impact of the SINR threshold

In this subsection, we examine the effect of SINR threshold, z on the success probability of the proposed model. In Fig. 4, we set $\lambda_R = 1$ Km/Km², $\mu_v = 10$ nodes/Km, $\lambda_b = 20$ BSs/Km² and $B = 1$. Fig. 4 plots the success probability of the V2X communication and V2V communication at the typical receiver versus the SINR Threshold. Following insights are observed: 1) The cellular V2X network performs better than V2V communication in the range of -20 dB to 20 dB SINR threshold because both V2V and V2B links are contributing in

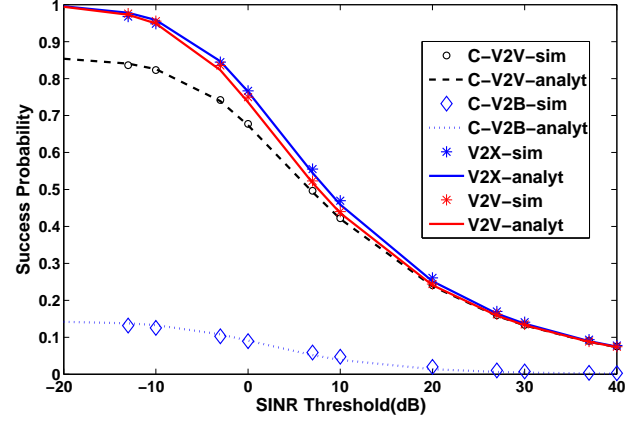


Fig. 4. The success probability versus the SINR threshold.

achieving the better reliability of V2X communication. However, after that, the success probability of V2X communication completely matches with V2V communication as there is no contribution by V2B link. 2) We see that the reliability advantage is more significant in V2X communication over V2V communication once vehicle intensities are low or medium. 3) We observe that in a highly dense V2X network, most of the vehicles connect via V2V link instead of V2B link.

B. Impact of the vehicle intensity

In this subsection, we examine the effect of vehicle intensity, μ_v at success probability and association probabilities of V2X network. In Fig. 5, 6, we set $\lambda_R = 5$ Km/Km², $\lambda_b = 20$ BSs/Km², $z = 0$ dB and $B = 1$.

Fig. 5 plots the success probability at the typical receiver versus the intensity of vehicular nodes. The following insights can be observed: 1) The success probability of V2X communication decreases as the intensity of vehicles on the roads increases due to decrease in V2B success probability. 2) In low and medium intensity networks, there is almost equal probability of connecting to V2V or V2B link. However, in highly dense networks, this advantage of cellular V2X communication over V2V communication reduces to certain extent. The success probability of V2X communication are still better than V2V communication. 3) We see that the cellular based V2V link success probability increases at faster rate with the increase of vehicle nodes. This is because of reduction in distance between the typical receiver and vehicle located on the lines that are closer to the origin. However, the distance between typical receiver and vehicles located on the lines that are farther away from the origin does not decrease at same rate due to effect of perpendicular distance of roads. This increases the desired signal power at a faster rate than the interference power, thus improving the SINR and hence the success probability at the typical receiver.

In Fig. 6, we plot the association probabilities of V2V and V2B links versus the intensity of vehicles. From the figure, we observed that with the increase of vehicular node intensities, more vehicles start to use the V2V link as the distance between

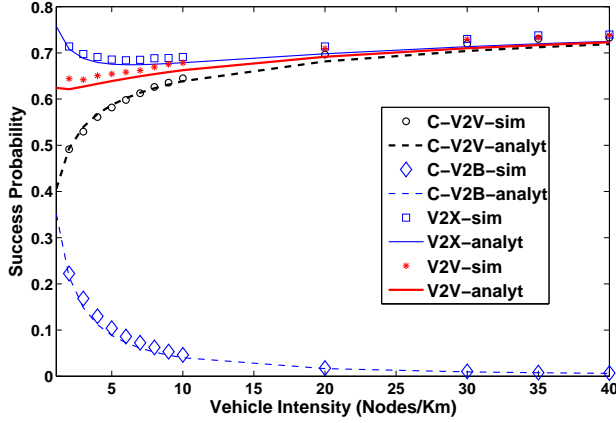


Fig. 5. The success probability versus the vehicle intensity.

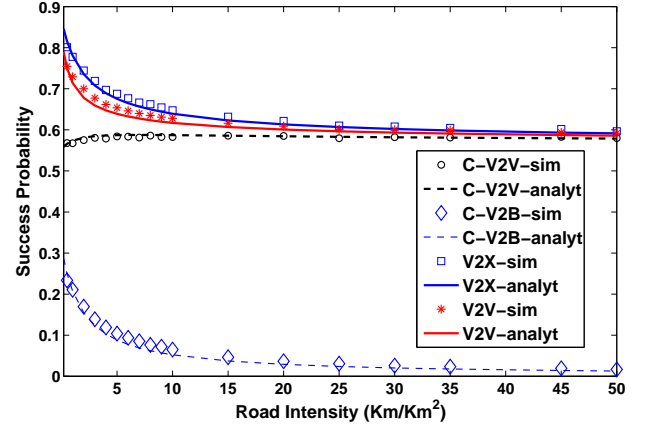


Fig. 7. The success probability versus the road intensity.

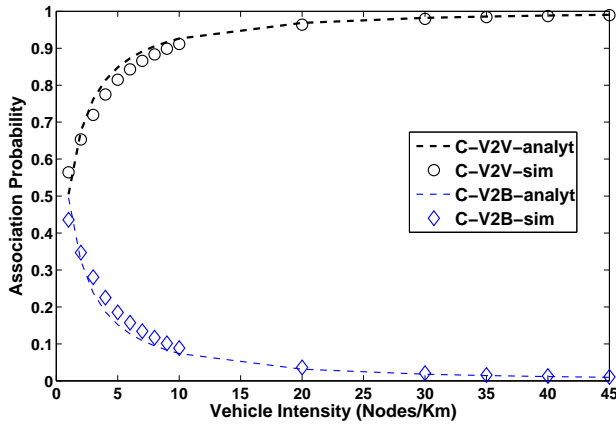


Fig. 6. The association Probability versus the vehicle intensity.

the vehicles reduces in highly dense network. On the other hand, in a low and medium intensity V2X networks, both V2V and V2B links are used by the vehicles.

C. Impact of the road intensity

In this subsection, we examine the effect of road intensity, Λ_R at packet success probability of V2X network and V2V communication. In Fig. 7, we set $\mu_v = 5$ nodes/Km, $\lambda_b = 20$ BSs/Km², $B = 1$ and $z = 0$ dB.

Fig. 7 plots the success probability at the typical receiver versus the intensity of roads. The following insights can be observed: 1) The success probability of V2X communication in low and medium intensities are much better than V2V communication. 2) In densely populated area with roads, the gain of V2X communication over V2V communication reduces. However, the success probability of the cellular V2X networks is still better than that of the V2V communication. From detailed analysis of results, we see that with the increase of road intensity, the V2V serving distance decreases by bring nodes closer due to which success probability increases and vehicles start using the V2V link instead of the V2B link.

D. Impact of the base-station intensity

In this subsection, we examine the effect of BS intensity, Λ_b at the success probability of the V2X communication and solely V2V communication. In Fig. 8, we set $\mu_v = 5$ nodes/Km, $\lambda_R = 5$ Km/Km², $B = 1$ and $z = 0$ dB.

Fig. 8 plots the success probability at the typical receiver versus the intensity of BSs. The following insights can be observed: 1) The success probability of cellular V2X network continuously increases at steady rate due to continuous rise in success probability of V2B link. 2) We observed that with the BS densification, the probability of having base-station in near vicinity to vehicular transmitter is higher than the PLP based V2V link distance, because the BSs are uniformly distributed instead of non-uniform PLP distribution of roads. 3) The success probability of the V2V communication remains constant as variation of BS intensities has no impact on V2V communication. 4) It is expected that in current heterogeneous networks where the intensity of BS is mostly high and sufficient, the number of cellular BSs are available to provide highly reliable coverage to vehicular networks. From this analysis, we can conclude that V2X communication is going to provide better reliability performance than V2V communication in current deployment scenarios of cellular networks.

E. Impact of the association bias

In this subsection, we examine the effect of association bias, B at packet success probability of V2X network and V2V communication. In Fig. 9, we set $\mu_v = 5$ nodes/Km, $\lambda_R = 5$ Km/Km², $\lambda_b = 20$ BSs/Km² and $z = 0$ dB.

Fig. 9 plots the success probability at the typical receiver versus the association bias. The following insights can be observed: 1) The success probability of V2X communication is much higher than V2V communication as both cellular based V2V and V2B links supplement each other for success probability of V2X communication and there are no coverage gaps for the network. 2) We observed that there is an increase in the success probability of the V2X communication with increase in values of bias, because the success probability of

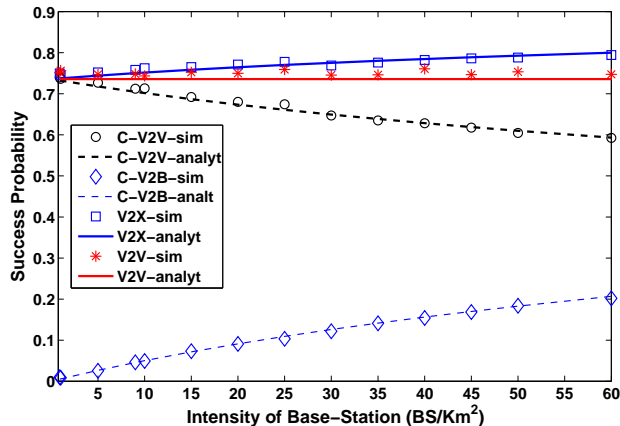


Fig. 8. The success probability versus the BSs intensity.

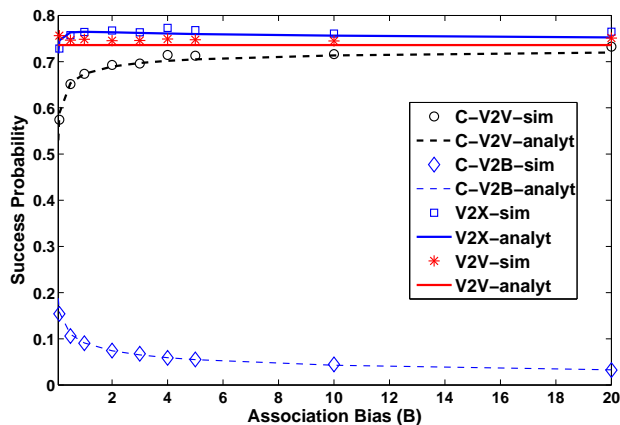


Fig. 9. The success probability versus the association bias.

V2V link initially increases at faster rate. 3) We see that at lower bias values, there is an equal opportunity for both links of being selected. At $B = 1$, there is equal probability of association with cellular based V2V or V2B link. 4) The success probability of V2V communication remains constant as association bias has no effect on this type of communication. 5) We can summarize that traffic loading and interference to cellular networks can be controlled through association bias.

VII. CONCLUSION

In this paper, we presented a comprehensive and tractable analytical framework for the reliability performance of cellular based vehicle-to-everything (V2X) communication in which vehicular communication can be established through cellular network or directly between vehicles on shared links. A flexible V2X uplink selection scheme has been proposed for the vehicular transmitter to decide between the vehicle to vehicle (V2V) and the vehicle to base station (V2B), with a bias factor controlling the amount of vehicular interference and traffic on the cellular network. By modeling the vehicles on roads as doubly stochastic Cox process, and the BSs as 2D PPP, we derived the expressions for the success probabilities

of the V2V link, the V2B link, as well as the V2X link, which are validated by the simulations. By comparing the proposed V2X communication with the solely V2V communication, we have shown the reliability enhancement brought by the shared communication via cellular networks. Future works can be extended to 1) interference mitigation techniques for cellular V2X network 2) the derivation of V2V communication analytical model for Ricean fading channel and results comparison with Rayleigh fading channels 3) modeling of vehicles on PLP as hard-core process on the line instead of PPP 4) implementation of the proposed model for vehicular communication and validation of reliability results of cellular V2X communication in comparison with V2V communication by the industry 5) correctness verification of using PLP for stochastic modeling the roads by using the Google maps and real roads.

APPENDIX A PROOF OF LEMMA 3

The conditional association probability of the V2V communication for shared link is given by

$$P_{v2v}^A(v2v|R_v) = P[B \times r_v^{-\alpha_v} \geq r_b^{-\alpha_b}], \quad (30)$$

where B is the association bias, r_v is the V2V link distance and r_b is the V2B link distance. By simplifying the above equation, we get

$$P_{v2v}^A(v2v|R_v) = P\left[r_b \geq \frac{r_v^{\frac{\alpha_v}{\alpha_b}}}{B^{\frac{1}{\alpha_b}}}\right]. \quad (31)$$

It means that the vehicular transmitter which is located at distance r_v is connected to vehicular receiver. Therefore, the radius of disk $b(0, \frac{r_v^{\frac{\alpha_v}{\alpha_b}}}{B^{\frac{1}{\alpha_b}}})$ does not contain any BS. By inserting CCDF of V2B link in (31), we get

$$P_{v2v}^A(v2v|R_v) = \exp\left(-\pi\lambda_B \left(\frac{r_v^{\frac{\alpha_v}{\alpha_b}}}{B^{\frac{1}{\alpha_b}}}\right)^2\right). \quad (32)$$

Now, removing condition on R_v , we get

$$P_{v2v}^A = \int_0^\infty \exp\left(-\pi\lambda_B \left(\frac{r_v^{\frac{\alpha_v}{\alpha_b}}}{B^{\frac{1}{\alpha_b}}}\right)^2\right) \times f_{R_v}(r_v) dr_v. \quad (33)$$

The PDF of R_v $f_{R_v}(r_v)$ is given in Eq. (5). The solution for the V2V association probability is proved in Eq. (7).

APPENDIX B PROOF OF LEMMA 4

The conditional association probability of the V2B shared link is given as

$$P_{v2b}^A(v2b|R_b) = P[B \times r_v^{-\alpha_v} < r_b^{-\alpha_b}]. \quad (34)$$

Simplifying the above equation, we get

$$P_{v2b}^A(v2b|R_b) = P\left[r_v > B^{\frac{1}{\alpha_v}} r_b^{\frac{\alpha_b}{\alpha_v}}\right]. \quad (35)$$

It means that the disk $b(0, B^{\frac{1}{\alpha_v}} r_b^{\frac{\alpha_b}{\alpha_v}})$ does not contain any vehicle, and thus

$$P_{v2b}^A(v2b|R_b) = P \left[\text{No vehicle in circle of radius, } B^{\frac{1}{\alpha_v}} r_b^{\frac{\alpha_b}{\alpha_v}} \right]. \quad (36)$$

By using the CCDF of R_v given in Eq. (3), we get

$$P_{v2b}^A(v2b|R_b) = \exp \left[-2\pi\lambda_R \int_{y_n=0}^{B^{\frac{1}{\alpha_v}} r_b^{\frac{\alpha_b}{\alpha_v}}} 1 - e^{-2\mu_v \sqrt{\left(B^{\frac{1}{\alpha_v}} r_b^{\frac{\alpha_b}{\alpha_v}} \right)^2 - y_n^2}} dy_n \right] \times \exp(-2\mu_v B^{\frac{1}{\alpha_v}} r_b^{\frac{\alpha_b}{\alpha_v}}). \quad (37)$$

Now, by removing condition on R_b and by inserting CDF of R_b in (37), we get Eq. (8) for the unconditional V2B shared link association probability.

APPENDIX C PROOF OF COROLLARY 2

The length of road R_{out} lying inside the circular region $\mathcal{B}(0, R)$ is $2\sqrt{R^2 - y^2}$ and distance between two vehicles can be denoted as t . By using the properties of a PPP, the probability of there being m points in this line segment can be calculated from 1D PPP. The conditional Laplace transform from these vehicles lying on this road segment to typical receiver can be calculated as follows

$$\mathcal{L}_{I_{R_{out}}}(s|r) = E_{D_x} \left[\prod_{x \in R_{out}} \left[\frac{1}{1 + sP_v D_x^{-\alpha}} \right] \right]. \quad (38)$$

Now conditioning over number of vehicles lying on the road and then deconditioning on interference caused by each node, we get

$$\mathcal{L}_{I_{R_{out}}}(s|r) = \sum_{m \geq 0} P[N_v = m] \times \left[\int_{-\sqrt{R^2 - y^2}}^{\sqrt{R^2 - y^2}} \frac{f(t) dt}{1 + sP_v (y^2 + t^2)^{\frac{-\alpha}{2}}} \right]^m. \quad (39)$$

The number of points on the line segment of length $2\sqrt{R^2 - y^2}$ is a Poisson random variable with mean $2\mu_v \sqrt{R^2 - y^2}$ and t is uniformly distributed between $(-\sqrt{R^2 - y^2}, \sqrt{R^2 - y^2})$ and has a PDF $f(t) = \frac{1}{2\sqrt{R^2 - y^2}}$.

By inserting pdf of $f(t)$ in the above equation, we get

$$\mathcal{L}_{I_{R_{out}}}(s|r) = \sum_{m \geq 0} \frac{e^{-2\mu_v \sqrt{R^2 - y^2}} (2\mu_v \sqrt{R^2 - y^2})^m}{m! (2\sqrt{R^2 - y^2})^m} \times \left[\int_{-\sqrt{R^2 - y^2}}^{\sqrt{R^2 - y^2}} \left(\frac{dt}{1 + sP_v (y^2 + t^2)^{\frac{-\alpha}{2}}} \right) \right]^m. \quad (40)$$

By simplifying above equation by using the property of integral of even function and by using the Taylor series expansion, $e^x = \sum_{n=0}^{\infty} \frac{x^n}{n!}$, we get

$$\mathcal{L}_{I_{R_{out}}}(s|r) = \exp \left(-2\mu_v \sqrt{R^2 - y^2} \right) \times \exp \left(2\mu_v \int_0^{\sqrt{R^2 - y^2}} \left(\left[\frac{dt}{1 + sP_v (y^2 + t^2)^{\frac{-\alpha}{2}}} \right] \right) \right). \quad (41)$$

The final expression for Laplace transform of interference from a road located outside the inner circular region $b(0, r)$ is given in equation (14).

APPENDIX D PROOF OF COROLLARY 3

We condition on number of roads, j crossing the region $\mathcal{B}(0, r)$ to calculate the interference from vehicles which lie on roads which interest the region $\mathcal{B}(0, r)$. However, on these lines, the interfering vehicles are located outside the region $\mathcal{B}(0, r)$. This is a Poisson random variable with mean $2\mu_v r \lambda_R$. Similarly, we condition on number of roads, k which lie between circular regions $\mathcal{B}(0, r)$ and $\mathcal{B}(0, R)$. This is also a Poisson random variable with mean $2\mu_v (R - r) \lambda_R$. Therefore, the Laplace Transform of interference of the total interference originating from Poisson Line Process can be written as

$$\mathcal{L}_{I_v}(s|r) = \left[\sum_{j \geq 0} \frac{\exp(-2\mu_v d \lambda_R) \times (2\mu_v r \lambda_R)^j}{j!} \times \left[\left(\int_{-r}^r \mathcal{L}_{I_{R1}}(s) \times f_Y(y) dy \right)^j \right] \right] \times \left[\sum_{k \geq 0} \frac{e^{-2\mu_v (R-r) \lambda_R} \times (2\mu_v (R-r) \lambda_R)^k}{k!} \times \left[\left(\int_{y=r}^R \mathcal{L}_{I_{R2}}(s) \times f_Y(y) dy \right)^k \right] \right]. \quad (42)$$

By writing the above equation in the form of Taylor series, we have

$$\mathcal{L}_{I_v}(s|r) = \left[e^{-2\mu_v r \lambda_R} \sum_{j \geq 0} \frac{\left(\mu_v \lambda_R \int_{y=-r}^r \mathcal{L}_{I_{R1}}(s) dy \right)^j}{j!} \right] \times \left[e^{-2\mu_v (R-r) \lambda_R} \sum_{k \geq 0} \frac{\left(\mu_v \lambda_R \int_{y=r}^R \mathcal{L}_{I_{R2}}(s) dy \right)^k}{k!} \right]. \quad (43)$$

By simplifying the above equation, we get the final result for Laplace Transform of interference of vehicles located on all roads excluding the road passing through the origin and it is proved in Eq. (20).

REFERENCES

- [1] 3GPP, "Document TR 36.885, study on LTE-based V2X services (release 14), technical specification group services system," *3GPP*, Jul. 2016.
- [2] J. Harding, G. Powell, R. Yoon, J. Fikentscher, C. Doyle, D. Sade, M. Lukuc, J. Simons, and J. Wang, "Vehicle-to-vehicle communications: Readiness of V2V technology for application," Tech. Rep., 2014.
- [3] K. Abboud, H. A. Omar, and W. Zhuang, "Interworking of DSRC and cellular network technologies for V2X communications: A survey," *IEEE Trans. on Veh. Tech.*, vol. 65, no. 12, pp. 9457–9470, Dec. 2016.
- [4] Y. Ren, F. Liu, Z. Liu, C. Wang, and Y. Ji, "Power control in D2D-based vehicular communication networks," *IEEE Trans. on Veh. Tech.*, vol. 64, no. 12, pp. 5547–5562, Oct. 2015.
- [5] K. Zheng, Q. Zheng, P. Chatzimisios, W. Xiang, and Y. Zhou, "Heterogeneous vehicular networking: a survey on architecture, challenges, and solutions," *IEEE commun. surveys & tutorials*, vol. 17, no. 4, pp. 2377–2396, Jun. 2015.
- [6] W. Sun, E. G. Ström, F. Brännström, Y. Sui, and K. C. Sou, "D2D-based V2V communications with latency and reliability constraints," in *GLOBECOM Wk.* IEEE, Dec. 2014, pp. 1414–1419.
- [7] T. D. Novlan, H. S. Dhillon, and J. G. Andrews, "Analytical modeling of uplink cellular networks," *IEEE Trans. Wireless Commun.*, vol. 12, no. 6, pp. 2669–2679, May. 2013.
- [8] J. G. Andrews, F. Baccelli, and R. K. Ganti, "A tractable approach to coverage and rate in cellular networks," *IEEE Trans. Commun.*, vol. 59, no. 11, pp. 3122–3134, Oct. 2011.
- [9] Y. Deng, L. Wang, M. ElKashlan, A. Nallanathan, and R. K. Mallik, "Physical layer security in three-tier wireless sensor networks: A stochastic geometry approach," *IEEE Trans. Inf. Forensics Security*, vol. 11, no. 6, pp. 1128–1138, Jan. 2016.
- [10] Y. Deng, L. Wang, S. A. R. Zaidi, J. Yuan, and M. ElKashlan, "Artificial-noise aided secure transmission in large scale spectrum sharing networks," *IEEE Trans. Commun.*, vol. 64, no. 5, pp. 2116–2129, Mar. 2016.
- [11] H. ElSawy, E. Hossain, and M. Haenggi, "Stochastic geometry for modeling, analysis, and design of multi-tier and cognitive cellular wireless networks: A survey," *Commun. Surveys Tuts.*, vol. 15, no. 3, pp. 996–1019, Jun. 2013.
- [12] Y. Deng, L. Wang, M. ElKashlan, M. Di Renzo, and J. Yuan, "Modeling and analysis of wireless power transfer in heterogeneous cellular networks," *IEEE Trans. Commun.*, vol. 64, no. 12, pp. 5290–5303, Dec. 2016.
- [13] H. ElSawy and E. Hossain, "On stochastic geometry modeling of cellular uplink transmission with truncated channel inversion power control," *IEEE Trans. Wireless Commun.*, vol. 13, no. 8, pp. 4454–4469, Aug. 2014.
- [14] M. N. Sial and J. Ahmed, "Analysis of k-tier 5G heterogeneous cellular network with dual-connectivity and uplink-downlink decoupled access," *Telecomm Systems*, pp. 1–17, Sep. 2017.
- [15] B. Blaszczyszyn, P. Mühlethaler, and Y. Toor, "Maximizing throughput of linear vehicular Ad-hoc NETWORKS (VANETs) a stochastic approach," in *Wireless Conf., EW 2009. European.* IEEE, May. 2009, pp. 32–36.
- [16] S. Busanelli, G. Ferrari, and R. Gruppini, "Performance analysis of broadcast protocols in VANETs with poisson vehicle distribution," in *Proc. ITST.* IEEE, Aug. 2011, pp. 133–138.
- [17] M. J. Farooq, H. ElSawy, and M.-S. Alouini, "A stochastic geometry model for multi-hop highway vehicular communication," *IEEE Transactions on Wireless Communications*, vol. 15, no. 3, pp. 2276–2291, Mar. 2016.
- [18] M. Mabilia, A. Busson, and V. Veque, "Inside VANET: hybrid network dimensioning and routing protocol comparison," in *Proc. VTC.* IEEE, Apr. 2007, pp. 227–232.
- [19] M. Ni, M. Hu, Z. Wang, and Z. Zhong, "Packet reception probability of VANETs in urban intersection scenario," in *Proc. ICCVE.* IEEE, Oct. 2015, pp. 124–125.
- [20] E. Steinmetz, M. Wildemeersch, T. Q. Quek, and H. Wymeersch, "A stochastic geometry model for vehicular communication near intersections," in *IEEE GLOBECOM Wks.* IEEE, Dec. 2015, pp. 1–6.
- [21] J. P. Jeyaraj and M. Haenggi, "Reliability analysis of v2v communications on orthogonal street systems," in *Proc. IEEE GLOBECOM.* IEEE, Dec. 2017, pp. 1–6.
- [22] Y. Wang, K. Venugopal, R. W. Heath, and A. F. Molisch, "Mmwave vehicle-to-infrastructure communication: Analysis of urban microcellular networks," *IEEE Transactions on Vehicular Technology*, 2018.
- [23] F. Voss, C. Gloaguen, F. Fleischer, and V. Schmidt, "Distributional properties of euclidean distances in wireless networks involving road systems," *IEEE J. Sel. Areas Commun.*, vol. 27, no. 7, Sep. 2009.
- [24] C. Gloaguen, F. Fleischer, H. Schmidt, and V. Schmidt, "Analysis of shortest paths and subscriber line lengths in telecommunication access networks," *Networks and Spatial Economics*, vol. 10, no. 1, pp. 15–47, 2010.
- [25] F. Morlot, "A population model based on a poisson line tessellation," in *Proc. Modeling and Optimization in Mobile, Ad Hoc and Wireless NW.* IEEE, May. 2012, pp. 337–342.
- [26] C. Gloaguen, F. Fleischer, H. Schmidt, and V. Schmidt, "Simulation of typical Cox-Voronoi cells with a special regard to implementation tests," *Mathematical Methods of Operations Research*, vol. 62, no. 3, pp. 357–373, 2005.
- [27] B. Blaszczyszyn and P. Mühlethaler, "Random linear multihop relaying in a general field of interferers using spatial aloha," *IEEE Trans. on Wireless Commun.*, vol. 14, no. 7, pp. 3700–3714, Jul. 2015.
- [28] V. V. Chetlur and H. S. Dhillon, "Coverage analysis of a vehicular network modeled as Cox process driven by poisson line process," *IEEE Trans. on Wireless Communications*, 2018.
- [29] S. Aditya, H. S. Dhillon, A. F. Molisch, and H. Behairy, "Asymptotic blind-spot analysis of localization networks under correlated blocking using a poisson line process," *IEEE Wireless Commun Letters*, vol. 6, no. 5, pp. 654–657, Oct. 2017.
- [30] S. Guha, "Cellular-assisted vehicular communications: A stochastic geometric approach," 2016.
- [31] C.-S. Choi and F. Baccelli, "An analytical framework for coverage in cellular networks leveraging vehicles," *IEEE Trans. on Commun.*, May. 2018.
- [32] F. Baccelli, M. Klein, M. Lebourges, and S. Zuyev, "Stochastic geometry and architecture of communication networks," *Telecommun. Systems*, vol. 7, no. 1-3, pp. 209–227, 1997.
- [33] S. N. Chiu, D. Stoyan, W. S. Kendall, and J. Mecke, *Stochastic geometry and its applications*, 2013.
- [34] Z. Tong, H. Lu, M. Haenggi, and C. Poellabauer, "A stochastic geometry approach to the modeling of DSRC for vehicular safety communication," *IEEE Trans. on ITS*, vol. 17, no. 5, pp. 1448–1458, May. 2016.
- [35] H. S. Jo, Y. J. Sang, P. Xia, and J. G. Andrews, "Heterogeneous cellular networks with flexible cell association: A comprehensive downlink SINR analysis," *IEEE Trans. Wireless Commun.*, vol. 11, no. 10, pp. 3484–3495, 2012.
- [36] H. ElSawy, E. Hossain, and M.-S. Alouini, "Analytical modeling of mode selection and power control for underlay D2D communication in cellular networks," *IEEE Trans. on Commun.*, vol. 62, no. 11, pp. 4147–4161, Nov. 2014.
- [37] F. Baccelli and B. Blaszczyszyn, "Stochastic geometry and wireless networks," *NOW Found. and Trends in Net.*, 2010.
- [38] H. S. Dhillon and J. G. Andrews, "Downlink rate distribution in heterogeneous cellular networks under generalized cell selection," *IEEE Wireless Commun. Ltrs.*, vol. 3, no. 1, pp. 42–45, 2014.